KERNFORSCHUNGSZENTRUM

KARLSRUHE

Oktober 1974 KFK 2069

Institut für Neutronenphysik und Reaktortechnik

# Cross Correlation of Neutronic and Acoustic Noise Signals from Local Boiling

S.A. Wright, R.W. Albrecht, M.F. Edelmann

GESELLSCHAFT
FÜR
KERNFORSCHUNG M.B.H.

KARLSRUHE

GESELLSCHAFT FÜR KERNFORSCHUNG M. B. H.

KARLSRUHE

KERNFORSCHUNGSZENTRUM KARLSRUHE

KFK 2069

Institut für Neutronenphysik und Reaktortechnik

# Cross Correlation of Neutronic and Acoustic Noise Signals from Local Boiling

S.A. Wright, R.W. Albrecht, and
M.F. Edelmann

Gesellschaft für Kernforschung mbH., Karlsruhe

---

Paper presented at the SMORN 1 EACRP Specialist Meeting on Reactor Noise, Rome, Italy, October 21-25, 1974

Abstract

A boiling simulator was constructed to model the void and pressure effects of local boiling in an LMFBR. By forcing superheated steam into subcooled water the boiling simulator produced a series of single bubbles separated by waiting times. The bubbles ranged from one to four centimeters in diameter and had lifetimes on the order of 60 milliseconds, and waiting times of 90 milliseconds. The boiling simulator was placed in the core of a zero power reactor (GfK, ARK), and the neutron and pressure signals were recorded and cross correlated. The neutron-pressure cross correlation exhibited an almost perfect correlation at the bubble repetition frequency (7 Hz). If (as expected) the normal pressure and reactivity background noises in a power reactor are uncorrelated, then this strong correlation will improve the signal-to-noise ratio of a boiling detection scheme. Other advantages of the cross correlation technique are that only simple linear transfer functions are necessary to relate the neutronic noise to the pressure noise and that the zone of the reactor (positive or negative void coefficient zone) can easily be determined. Because of these advantages, the neutron-pressure cross correlation technique is considered a serious alternative for the detection of local boiling in sodium cooled reactors.

# Kreuzkorrelation zwischen Rauschsignalen aus Neutronendetektoren und Schallaufnehmern bei lokalem Sieden


## Zusammenfassung

Zur Nachbildung von lokalen Siedevorgängen in einem Flüssigmetall-gekühlten Brutreaktor wurde ein Siedegenerator entwickelt, mit dem in einem wassermoderierten Nulleistungsreaktor (Argonaut) die für Na-Sieden typischen Reaktivitäts- und Druckeffekte simuliert werden konnten. Durch Einleitung überhitzten Wasserdampfes in Wasser wurden Folgen von Einzelblasen mit einem Durchmesser zwischen 1 und 4 cm, einer Lebensdauer von größenordnungsmäßig 60 ms und Folgefrequenzen zwischen 7 und 20 Hz erzeugt.

Die Druck- und Neutronenflußschwankungen im Reaktor wurden gemessen und spektral analysiert. Die spektrale Kreuzleistungsdichte zeigt bei der Blasenfolgefrequenz eine Resonanz. Die beiden Signale sind bei dieser Frequenz stark korreliert. Daher ist es möglich, das Signal-zu-Untergrundverhältnis beim Siedenachweis durch Kreuzkorrelation von Neutronen- und Drucksignalen zu verbessern. Der Zusammenhang dieser Signale konnte durch einfache Übertragungsfunktionen eines linearen Modells beschrieben werden. Die Untersuchungen zeigten, daß die Kreuzkorrelation von Druck und Neutronenfluß eine erfolgversprechende Grundlage für den Nachweis lokalen Siedens in Natrium-gekühlten Reaktoren bietet.

## Introduction

The local loss of coolant in an LMFBR is one of the most important safety problems for reactor design and operation. The accident is considered important because of its potential for serious damage and its "finite probability" of occuring /1/. The accident is initiated either by a blockage or pump failure. Depending upon the size of blockage, local or integral boiling will occur. For integral boiling, failure of the fuel cladding occurs because of continuous loss of coolant, or "dryout". In the case of local boiling, damage can occur as a result of long time exposure to periodic overheating. Definitely for integral boiling and possibly even for local boiling, fuel melting quickly follows the cladding failure and results in a violent reaction between the overheated sodium and molten fuel. It is feared that the pressure pulse from the sodium fuel interaction could cause the accident to propagate throughout the entire core.

In principle, the above series of events can be stopped following detection of one or more of the events causing boiling or caused by boiling, i.e. loss of flow, temperature increases, pressure impulses, and reactivity effects. Because heavy instrumentation of individual subassemblies is not compatible with economic reactor design, it is necessary to use a detection scheme which is global. That is, one that can survey the entire reactor core or at least large portions of it.

Acoustic and neutronic noise methods are the primary methods considered probable to provide such a global surveillance of sodium boiling. Both of these methods, however, have serious signal-to-noise problems due to background noise sources present in the reactor. Because the background noise sources for the two signals are physically different in most cases, a strong correlation between them should not exist. Thus cross correlation of the neutron and pressure signals will improve the signal-to-noise ratio provided the portion of the neutron

and pressure signals caused by boiling are strongly correlated. Since a pressure impulse always occurs at the collapse of each bubble (in local boiling), a strong correlation at the bubble repetition frequency can be expected. These two facts, no or weak correlation of background noises and strong correlation of the boiling-produced signal motivated a boiling experiment in which neutronic and pressure noise signals caused by local boiling were simulated in a nuclear reactor and cross correlated.

## Sodium Boiling Dynamic Characteristics

Boiling, consisting of a two phase mixture of vapor and liquid like that in water, is almost impossible in sodium because of the existence of high superheat and the lack of nucleation sites /2/. Instead, large single bubbles are formed in a rapid vaporization process. The bubbles later collapse due to an increased condensation rate brought on by expansion of the bubble into cooler regions of the coolant.

A great deal of theoretical and experimental work has been devoted to the determination of sodium boiling characteristics /2,3,4,5/. This literature indicates that only integral and local boiling are likely to occur in sodium cooled reactors.

Integral boiling /2/ is initiated by a total or almost total blockage of a subassembly or by loss of coolant flow due to pump failure. Regardless of the initiating event, boiling begins a few tenths of a second after the coolant flow rate has been reduced to approximately 10% the normal flow rate, at which point cladding failure also begins. The entire cross section of the subassembly is voided to many tens of centimeters above the blockage, provided the initiating event is a blockage. If the initiating event is pump failure or blockage below the subassembly inlet, then the void occurs about a position slightly above the reactor midplane. In some cases the boiling void can expand out of the core region into the blanket. The void volume oscillates in the frequency range from 2-5 Hz with only the first few bubbles collapsing completely. Because of the

incomplete collapse, "dryout" of the thin sodium film coating the fuel elements occurs. This results in fuel melting within 3-5 seconds. This type of boiling is also known as chugging.

In contrast to integral boiling, the initiating event for local boiling /3/ is a partial blockage of a subassembly. Large single bubbles grow and collapse over a partial cross sectional area of the subassembly while coolant flow continues around the blockage. The bubbles take on the shape of a half sphere pierced by the fuel elements and have maximum radii from 1 to 4 centimeters and lifetimes of 30 to 60 milliseconds. The bubbles collapse completely. At the end of each collapse a large pressure pulse is created. Following the collapse of the first bubble and the growth of the next, a waiting time may occur depending upon the value of the superheat at which the next bubble is formed. However, no such waiting time has been observed in sodium boiling experiments. (This discrepancy between experiment and theory still needs to be resolved /4/.) Depending upon whether or not a waiting time occurs, the bubbles will have a repetition frequency from 6 to 30 Hz. Dryout does not occur because the bubbles fully collapse. However, sufficient temperature rise of the cladding can occur to cause damage and thus lead to a more severe type of boiling accident as a result of fuel or other solid particels sweeping through the coolant loop and increasing the size of the blockage /4/ or gas blanketing caused by pinhole failures in the cladding /1/.

The differences in the two types of boiling will have a definite effect on the type of detection method used. Because only small blockages are required to cause local boiling, deposits can build up on the fuel element spacers over a long period of time. In addition to the blockage causing a decrease in flow, a coolant recirculation region is formed behind the blockage. In the region behind the blockage, heat transfer is hindered causing an increase in coolant and fuel element temperatures. If the temperature rise is high enough, boiling will occur. This slow build-up of a small blockage is thought to be more probable than the large sudden blockage required for integral boiling. Consequently, the occurrence of local boiling is more probable than integral boiling /3,4/.

The spatial dependence of the reactivity void coefficient in LMFBR's will have a large effect on the reactivity perturbations produced by the two boiling types. Because LMFBR's have a zone with zero void coefficient, no reactivity effect can be expected if local boiling occurs in this region. However, the large size of the bubbles from integral boiling will always produce some reactivity effect. Thus a portion of the reactor will be left unprotected with respect to local boiling detection, if the boiling detection is dependent only upon void created reactivity effects.

Probably the greatest difference between the detection of the two boiling types is that simple temperature and flow transducers placed at the exit of each subassembly will not be able to detect local boiling initiated by blockages less than 1/3 the subassembly cross section /1,3,4/; the boiling signals will be obscurred by background noises. Hence the detection of local boiling in this manner will be very difficult.
Finally, a last observation is that despite the small size of the bubbles, there is still potential for reliable detection. This is true for two reasons. First, since dryout does not occur in local boiling, a longer time will be available for observation before damage occurs. Second, since the bubble repetition frequency is higher for local boiling, more bubbles will be observed in a specified time than for integral boiling. This fact reduces the variance which increases the detection reliability.
There are also some common problems which the detection of any anomaly type must overcome. As already stated, a practical detection method must use a global surveillance technique. Also it must be rapid and reliable with few or no false detections. Durable and sensitive detectors must be used. And finally, detection of the anomaly must be achieved despite the lack of detailed knowledge of the position and type of initiating event.

A summary of the above ideas shows that local boiling:

1. has a higher probability of occurring than integral boiling,
2. will be difficult to detect using simple temperature and flow transducers,
3. and has a high potential for damage.

These facts indicate that the development of a global surveillance system to rapidily and reliably detect local boiling would be constructive for the safe and economic operation of a sodium cooled reactor. Already, considerable work has gone into the understanding and detection of integral boiling /1,2, 5,6/. This paper addresses itself to the detection problem of local boiling, specifically (as mentioned in the introduction) to the problem of using cross correlation methods between acoustic and neutronic noise.

## Experimental Set-Up to Simulate Local Boiling

Because of the difficulties in performing true boiling experiments in sodium cooled reactors, most of the experimental effort thus far has been directed toward the simulation of prototypical boiling in out-of-core test sections and in the cores of water cooled research reactors. In-core experiments have of necessity been less prototypical (with respect to reproducing the boiling characteristics) than out-of-core experiments. This is due to a number of factors, including the lack of instrumentation available in the boiling element, confined space, and the hostile environment in which the simulator must operate. The first in-core experiments often consisted of bubbling an inert gas through the core, submerging some kind of heating element into the coolant, or orificing a subassembly. Often the detailed dynamic characteristics of these boiling simulators were not known /7/.

To overcome the above drawbacks, a boiling experiment was designed whose detailed characteristics could be directly observed in out-of-core experiments. The boiling generators main purpose was to

reproduce the void and pressure charactersitics of local boiling. Once the proper boiling characteristics were established, the generator was placed in the core of a zero power reactor. The global neutronic and acoustic noise signals were recorded and later compared to the out-of-core data. A description of the boiling generator and the in-core and out-of-core experiment follows.

The boiling generator simulated the void and pressure effects of local boiling by forcing superheated steam into subcooled water through a nozzel (see figure 1). A series of single bubbles was produced whose size and lifetime could be varied by changing the water temperature. Typical bubble diameters and lifetimes varied from 1 to 6 cm and 30 to 60 msec, respectively.

Figure 1 shows a schematic diagram of the boiling simulator. It consists of two parts, a steam generator and a water column into which the steam is injected. The steam generator is capable of supplying steam at 150 $^{o}$C and 5 atm with a mass flow rate of 2-3 gm/sec. The water column is contained inside a 2 meter long clear plexiglass tube and has a diameter of 10 cm. The water is kept at constant temperature by circulating cool water through a long stainless steel tube submerged in the water column. A thermocouple measures the water temperature in the vicinity of the nozzel while a piezoelectric pressure transducer (Kistler 701A), placed at the top of the water column, monitors the pressure noise. (In this report pressure noise and acoustic noise will be used interchangeably.)

In the out-of-core experiments, high speed films of the bubble growth and collapse were made. Simultaneously, the pressure signals were recorded on magnetic tape. Time marks on both the films and tape recordings made possible synchronization of the bubble volume with the pressure.

The in-core experiments were performed in the zero power (10 Watt) GfK reactor, ARK. This reactor is an argonaut type with a ring type fuel zone. The fuel plates of one subassembly were removed and distributed in the other subassemblies, and the boiling simulator was placed in the emptied subassembly. Figure 2 shows a top view of the reactor and the position of the boiling simulator. Using the reactor period technique, the void coefficient in the boiling zone was measured and found to be +11m¢/ccm (±2m¢/ccm).

The in-core instrumentation consists of two $He^3$ neutron detectors placed in the thermal column of the reactor and one pressure transducer located at the top of the water column. The neutron and pressure signals were recorded on an Ampex FM tape recorder.

Figure 3 shows a schematic diagram of the analysis equipment. The two neutron signals were D.C. compensated, preamplified, bandpass filtered (0.2 - 2000 Hz), and then recorded. The pressure signal was preamplified by a specially designed Kiag charge amplifier and then directly recorded. The auto and cross power spectral densities were calculated with a spectral analyzer consisting of an ADC, Hewlett Packard model 2116B computer, and a specially designed fast fourier transform unit.

## Theory

A detailed analysis (noise analysis) of the statistical fluctuations that occur in a system's output signals will contain information about the system as well as the system's driving forces. The use of noise analysis has the advantage that it allows observation of a system without externally perturbing the system. However, when external perturbations do occur, it will be very sensitive to these perturbations. For these reasons, noise analysis is considered an excellent tool to detect the

occurrence of anomalies in nuclear reactors.

The Power Spectral Density (PSD) and correlation function are the functions generally used in noise analysis to display the information. The PSD is a measure of the average power a signal contains at some frequency per unit bandwidth about this frequency, and the correlation function is a measure of the averaged product that two points of a signal separated by a delay time take on. Only the PSD will be used in the theoretical development described in this section. The Auto Power Spectral Density (APSD) and Cross Power Spectral Density (CPSD) for two stationary signals $x(t)$ and $y(t)$ with zero mean are defined as /8/.

$$\text{APSD} = S_{xx}(\omega) = \lim_{T \to \infty} \frac{E[X(j\omega)\, X^*(j\omega)]}{T} \qquad (1)$$

$$\text{CPSD} = S_{xy}(\omega) = \lim_{T \to \infty} \frac{E[X(j\omega)\, Y^*(j\omega)]}{T} \qquad (2)$$

where $X(j\omega)$ and $Y(j\omega)$ are the fourier transforms of $x(t)$ and $y(t)$ respectively. The star $*$ signifies the complex conjugate, and $E[\ ]$ signifies the ensemble average. If the signals are ergodic, then the PSD's can be estimated by long but finite time averages rather than ensemble averages.

$$S_{xx}(\omega) \approx \frac{\langle X(j\omega)\, X^*(j\omega) \rangle}{T} \qquad (3)$$

$$S_{xy}(\omega) \approx \frac{\langle X(j\omega)\, Y^*(j\omega) \rangle}{T} \qquad (4)$$

The symbol $\langle\ \rangle$ signifies time averaging over time T.

For the purpose of this report, a nuclear reactor will be considered a system driven by two external input noise sources and having neutronic and acoustic noise signals as outputs. The two input noise sources are the boiling process and the background power noise. The latter exists in all power reactors. This power noise arises from a variety of sources such as vibrations, pump noise, inlet coolant temperature fluctuations, coolant turbulence, etc. In general, the power noise sources for the neutronic noise and acoustic noise are different. Table 1 lists the various neutronic and acoustic noise sources.

Figure 4 shows a block diagram of the reactor system. It is seen that there are two paths connecting the various inputs to the outputs, one path for the neutronic output signal and one path for the acoustic signal. For each path the APSD will be calculated as well as the combined CPSD. From the derived PSD equations and the assumptions necessary to derive them, some simple but important conclusions can be made.

In the neutronic path of the reactor system, the oscillating bubble volume produces a reactivity input, $\rho_B(\omega)$, by means of the spatially dependent void coefficient, $\alpha_v$ . In addition to the boiling reactivity input, there will be inputs caused by the reactor power noise, $\rho_L(\omega)$ . Finally there will be contributions to the signal fluctuations as measured by a neutron detector through the "zero power" fission chain noise source $\delta(\omega)$ and the detector noise $\eta(\omega)$ . By considering the input noises, and the reactivity transfer function $H(\omega)$ , and the APSD definitions, one can derive the neutron APSD, $S_{N'N'}(\omega)$ /9/.

$$S_{N'N'}(\omega) = W\bar{q}^2 FR + W^2\bar{q}^2 FD|H(\omega)|^2 + W^2\bar{q}^2F^2|H(\omega)|^2 S_{\rho\rho}(\omega) \qquad (5)$$

where *

$W$ is the detector efficiency in det./fis.

$F$ is the total fission rate

$\bar{q}$ is the mean electric charge collected per detection

$R = \overline{q^2} / \bar{q}^2 \approx 1.2$

$D = \overline{\nu(\nu-1)} / \bar{\nu}^2 \approx 0.8$ , Diven factor

$S_{\rho\rho}$ is the APSD of the total reactivity input

$H(\omega)$ is the one group point reactor model reactivity transfer function including feedback. If feedback is neglected it equals $\frac{j\omega+\lambda}{\Lambda j\omega(j\omega+\beta/\Lambda)} \approx \frac{1}{j\omega\Lambda+\beta}$ for $\omega \gg \lambda$ .

The first part of equation 5 is commonly called the detection noise term and arises because of the statistical fluctuations in the charge collected per neutron detected in the detector. The second portion is called the fission noise term, and results from the fluctuations of the fission chain branching process. Finally, the third term, which is generally called power noise term, is caused by the external reactivity perturbations such as boiling or normal power noise. For power reactors this term will dominate the first two terms because it is proportional to the square of the power. In this last term the APSD of the external reactivity perturbations, $S_{\rho\rho}(\omega)$ , can be represented in terms of the bubble volume and power noise auto and cross PSD's.

$$S_{\rho\rho}(\omega) = \alpha_v^2 \, S_{vv}(\omega)\Big|_B + S_{\rho\rho}(\omega)\Big|_L + 2\,\mathrm{Re}\{S_{\rho\rho}(\omega)\}\Big|_{BL} \qquad (6)$$

The last term of this equation is twice the real part of the cross correlation between boiling and power noise. Because boiling can occur independently of the background power noise, it is reasonable to assume that the normal power noise is

* All other terms are defined in the appendix.

uncorrelated with the boiling noise, consequently making the last term negligible. This is a conservative assumption with respect to boiling detection because any correlation would tend to improve the signal-to-noise ratio.* Equation 6 can be simplified to

$$S_{pp}(\omega) = \alpha_v^2 \, S_{vv}(\omega)\Big|_B + S_{pp}(\omega)\Big|_L \qquad (7)$$

This equation together with equation 5 determines the APSD of the neutron fluctuations for a power reactor.

In addition to acting as a driving force for the neutron population, the boiling also serves as a driving force for the acoustic noise, $P_B(\omega)$ . The driving force acts through the acoustic path of the reactor system having as a main component the volume-pressure transfer function $H_p(\omega)$ . This transfer function can be estimated by using the Euler and continuity equations of fluid dynamics. The pressure p at a distance r is calculated for a spherical bubble growing in an infinite sea of liquid. The resulting equation is linearized by neglecting a term which falls off at $1/r^4$ while keeping the dominate term which is proportional to 1/r. The result is

$$p(t) = \frac{\rho_d}{4\pi r} \cdot \frac{\partial^2 v(t)}{\partial t^2} \qquad (8)$$

where $\rho_d$ is the liquid density,
$v(t)$ is the time dependent bubble volume, and
$r$ is the distance from the bubble to the detector.

This equation is easily Laplace transformed to obtain the transfer function $H_p(\omega)$ .

$$H_p(\omega) = \frac{P_B(\omega)}{V(\omega)} = \frac{-\omega^2 \rho_d}{4\pi r} \qquad (9)$$

*Provided boiling-induced and correlated power noise are essentially in phase.

As a first approximation the above equation will be used, regardless of the fact that the actual experiment did not use spherical geometry.

Along with the boiling induced pressure noises, there will also be the background pressure noise sources, $P_L(\omega)$ . Applying the APSD definitions to the two input sources and using the volume-pressure transfer function the pressure APSD $S_{PP}(\omega)$ can be derived.

$$S_{PP}(\omega) = \frac{\rho_d^2 \omega^4}{(4\pi r)^2} \; S_{VV}(\omega)\Big|_B + S_{PP}(\omega)\Big|_L + 2\,\mathrm{Re}\{S_{PP}(\omega)\}\Big|_{BL} \tag{10}$$

The first term of this equation is the boiling induced noise, the second term is the normal background pressure noise, and the last term results from the cross correlation between boiling noise and background noise. Again this last term can be neglected because there is probably very little correlation. (As previously mentioned this is a conservative assumption with respect to boiling detection.) Because of this fact the APSD then takes on the following more simple form

$$S_{PP}(\omega) = \frac{\rho_d^2 \omega^4}{(4\pi r)^2} \; S_{VV}(\omega)\Big|_B + S_{PP}(\omega)\Big|_L \tag{11}$$

From the above equations and the assumptions necessary to derive them, the following statements can be made regarding the acoustic and neutronic PSD's.

1. For a typical power reactor, the external reactivity noises due to boiling and normal background noise will dominate the detection and fission chain noise in the neutron APSD.

2. Simple linear transfer functions exist which relate the oscillating bubble volume to the neutron and pressure fluctuations. As a consequence, the neutronic and pressure noise should be strongly correlated.

3. The pressure APSD due to boiling will have considerable high frequency contributions because the volume-pressure transfer function $H_p(\omega)$ is proportional to $\omega^2$ . In practice this is an over-simplification; the existance of dissolved gases and geometry effects will severely effect the pressure propagation through the liquid medium.

4. The neutron APSD is spatially dependent because of the spatial dependence of the void coefficient.

5. The pressure APSD is also spatially dependent and depends on the separation between the bubble and detector. For spherical geometry it is proportional to $1/r^2$ . In practice the situation will be much more complicated because of geometry effects.

6. The assumption that the boiling volume oscillations are not correlated with the normal background reactivity and pressure noise is conservative. The existence of any such correlation can only aid boiling detection (cf. footnote on p.11).

Since boiling acts as a driving force through both the pressure and neutronic reactor transfer function paths, the neutronic and acoustic noise should be correlated. Applying the CPSD definitions, one obtains the neutron-pressure CPSD, $S_{N'P}(\omega)$.

$$S_{N'P}(\omega) = W\bar{q}F\,H(\omega)\left\{ S_{PP}(\omega)\Big|_L + \alpha_v H_P^*(\omega)\, S_{VV}(\omega)\Big|_B \right\} \qquad (12)$$

It has been assumed that the boiling induced noise is uncorrelated with the background noise. Since $S_{VV}$ is not directly measurable except through the films, a more useful expression is obtained by putting the CPSD in terms of $S_{pp}$ . The result is

$$S_{N'P}(\omega) = W\bar{q}F\,H(\omega)\left\{ S_{PP}(\omega)\Big|_{L} + \frac{\alpha_V}{H_P(\omega)}\; S_{PP}(\omega)\Big|_{B}\right\} \quad (13)$$

The first term represents the cross correlation between the background reactivity noise and pressure noise, and the second term represents the boiling induced cross correlation. The first cross correlation term should be small or zero because the sources for each noise type are physically different (see table 1). Certainly, for a zero power reactor, where there are no external background noise sources (reactivity or pressure), this term will be zero. The CPSD thus becomes

$$S_{N'P}(\omega) = W\bar{q}F\,\alpha_V\,\frac{H(\omega)}{H_P(\omega)}\; S_{PP}(\omega)\Big|_{B} \quad (14)$$

If one substitutes into this equation, the zero power point reactor transfer function, and the volume-pressure transfer function one obtains

$$S_{N'P}(\omega) = \frac{W\bar{q}F\alpha_V 4\pi r}{\rho_d \Lambda} \cdot \frac{-1}{\omega^2(j\omega+\beta/\Lambda)}\; S_{PP}(\omega) \quad (15)$$

From this equation some very important observations can be made.

1. The neutron-pressure CPSD is spatially dependent and depends on the bubble pressure detector separation and the reactivity void coefficient.

2. If (as expected) the background reactivity and pressure noise of power reactors is caused by independent physical driving sources, the CPSD will have no background noise term to compete with the boiling induced term.

3. The pseudo transfer function, $S_{N'P}(\omega) / S_{PP}(\omega)$ is proportional to $1/\omega^2$ below the break frequency of the reactor $(\beta/\Lambda)$ and to $1/\omega^3$ above the break frequency.

4. Because the CPSD is proportional to the void coefficient, a change in its sign will be apparent as a $180^{\circ}$ phase shift in the phase angle. Thus it will be possible to determine in which zone (i.e. positive or negative void coefficient) the boiling occurs. Table 2 shows the CPSD phase angle as a function of void coefficient zone and frequency.

From the theoretical work described above it is clear that the neutron-pressure CPSD has two advantages over either the neutron or pressure APSD. These are the improvement in the signal-to-noise ratio, caused by the decreased background noise and high correlation in the boiling induced noise, and the ability to determine in which reactor zone boiling occurs.

## Experimental Results and Comparison with Theory

The out-of-core experiments provided a direct observation of the bubble cross sectional area. Figure 5 shows the bubble volume time dependence for a typical series of bubbles (as determined from the high speed films) and the synchronized pressure signals. The volume was calculated from the cross sectional areas by assuming spherical bubbles. A detailed look at the bubble volume time history reveals that in most cases a small bubble first forms and then partially collapses followed immediately by a much larger bubble. Following this "2-bubble" pattern, a waiting time exists before the growth of the next bubble pattern. Occurring simultaneously with the bubble collapse is a double impulse in the pressure signal. The first portion of the impulse is negative going, caused by the rapidly collapsing bubble. The second portion is positive going and is due to the clapping together of the liquid surface filling the void. There is some evidence that in liquid sodium

the collapse rate will be much slower thus eliminating the negative going peak /6/.

The bubble volume was controlled by varying the water temperature into which the steam was injected. Bubble volumes ranging from 15 $cm^3$ to 120 $cm^3$ were produced. The bubble lifetimes were on the order of 60 msec and the waiting times 80 msec. This resulted in repetition frequencies of 7 Hz. Alterations in the water temperature affected the bubble repetition frequency only slightly because any increase in the bubble lifetime was accompanied by a corresponding decrease in the waiting time.

In general, the out-of-core experiments indicate that the boiling generator satisfactorily simulates the volume and pressure effects of local boiling. The existence of the 2-bubble pattern and waiting time does not seriously affect the prototypicality of the simulation. In fact, these effects might even be characteristic of true sodium boiling. In some of the sodium boiling experiments performed by Schleisiek /6/, a 2-bubble pattern can be observed. The existence of waiting times, though never directly observed by Schleisiek, are predicted by some theories. However, the real problem is that no dynamic bubble theory exists which is valid for a series of bubbles. They are valid only for the first bubble produced after the blockage occurs.

The comparison of the theory with the experimental results should use both the out-of-core data and the in-core data. For the out-of-core experiment, only the volume-pressure transfer function can be checked. This was done in the time domain by differentiating the bubble volume twice (as observed from the films) and comparing the resulting shape with the experimentally observed pressure signal. See figure 6 for the results. No attempt was made to determine the magnitudes since the model is valid only for spherical geometry and cylindrical geometry should be applied. Despite the very "noisy" double differentiating process, the simple model does an acceptable

job of predicting the position and relative magnitude of each pulse. It even reproduces the double impulse pattern of the negative and positive going pulses.

Several different boiling cases were simulated in the in-core experiments. These include at least six different bubble volumes and in addition two non-boiling cases. For the non-boiling cases, the reactor was controlled manually and automatically. This was done to determine if the automatic control had any strong effects in the neutron APSD. None were observed. For a typical boiling case with bubble volumes of 32 $cm^3$ and a water temperature of $71^{o}$ C, the neutron and pressure APSD's and CPSD are shown in figures 7, 8, and 9. With the aid of the out-of-core experimental results, it was possible to identify many of the observed peaks in these PSD's. Before explaining the peaks in detail, some general remarks are in order. Most of the power in the pressure APSD is below 200 Hz. This is probably a result of the damping caused by the large amount of dissolved gas in the water column. Only the peaks below 30 Hz will be discussed in detail because they are directly related to the bubble growth and collapse. Peaks above this frequency are probably more correlated with the resonance frequencies of the test column and its physical construction rather than with the bubble dynamic characteristics.

Three peaks are apparent in the pressure APSD (see figure 7). The first, at 7 Hz, is due to the large bubble repetition frequency, and the second, at 14 Hz, is also associated with the bubble repetition frequency. This second peak is at twice the large bubble repetition frequency because of the 2-bubble pattern. The third peak, at 23 Hz, is caused by the duration of the pressure impulse. It was observed that the higher frequency peaks ($>$30 Hz) decreased in amplitude with increasing water temperatures, while the lower frequency peaks (especially the large bubble repetition frequency) increased with increasing water temperatures. This indicates that these higher frequency peaks are also related to the bubble collapse, since the collapse rate depends on the water temperature. Also, all peaks shifted to slightly lower frequencies for increases

in water temperature.

The neutron APSD (figure 8) exhibits only the peak at the large bubble repetition frequency (7 Hz). This occurs because the reactivity transfer function of the reactor has in effect a low pass filter characteristics with break frequency at 6Hz. Thus, the 2-bubble pattern appears only as one large bubble (hence the term, large bubble repetition frequency). Increases in the bubble volume caused increases in the peak value of the large bubble resonance. For very small bubbles the neutron APSD differs only slightly from the non-boiling case. A detection scheme based solely on the neutron APSD would have difficulty in detecting the boiling event for this case.

The neutron-pressure CPSD (figure 9) has a very narrow band peak at the large bubble repetition rate. Peaks are also seen at the 2-bubble repetition frequency and at the pressure pulse duration time. The correlation between the bubble volume and pressure at these last two frequencies were not apparent by observing the APSD's, however they are shown clearly in the CPSD.

As observed in the theoretical section of this paper, it should be possible to determine the sign of the void coefficient from the CPSD phase diagram. For a positive void coefficient, the phase angle should be $180^{\circ}$ for frequencies less than the break frequency $(\beta/\Lambda)$ and $90^{\circ}$ for frequencies greater than the break frequency. This effect is observed in the phase diagram plotted in figure 9. The fact that the phase does not quite approach $90^{\circ}$ might be corrected if the simple spherical geometry model for $H_p(\omega)$ had not been used. For frequencies greater than 30 Hz, no correlation between the neutron and pressure signal exists, thus no confidence can be placed in the value of the phase angle.

The previous statements on the phase angles serve as a partial check for the model relating bubble volume to pressure using the out-of-core data. A further check is obtained by looking at the shape of the CPSD. This is most easily done by dividing

equation (15) by the pressure APSD to obtain

$$\frac{S_{N'p}(\omega)}{S_{pp}(\omega)} = \frac{W\bar{q}F\alpha_v 4\pi r}{\rho_d \Lambda} \cdot \frac{-1}{\omega^2(j\omega + \beta/\Lambda)} \qquad (16)$$

The left hand side of this equation is purely experimental while the right hand side is theoretical. Figure 10 shows a plot of the measured curve and the theoretical curve. The absolute magnitude of the theoretical value has been normalized to fit the experimental value at the break frequency of the reactor. For frequencies above the break frequency it is seen that both the theoretical and experimental curves fall of at $1/\omega^3$ . The slight difference in slope is probably due to the spherical geometry model used. The lack of agreement between theory and experiment at the low frequencies is probably caused by the combined effect of the lower cut-off frequency of the pressure transducer and the lack of correlation between the neutronic and pressure noise in this frequency range.

Coherences of the neutron-pressure cross correlation were also made (see figure 11). For the case described in this paper, a coherence of 0.6 was measured at the bubble repetition frequency. When one takes into account the detection and fission noise, this indicates an almost perfect correlation between the bubble volume and pressure. This fact, along with the in-core and out-of-core results, indicates the validity of the simple linear model relating bubble volume to pressure.

## Summary and Conclusions

The experimental investigation set out to show that local sodium boiling causes the neutronic and pressure signals to be strongly correlated. The existence of such a correlation is significant because the cross correlation of neutron and pressure signals will result in a better signal-to-noise ratio than either the neutron or pressure APSD's.

As a result of this experiment, the following conclusions can be made

1. There is almost a perfect correlation between the bubble volume and pressure at the bubble repetition frequency for local boiling.

2. Only simple models are required to relate the bubble volume to the pressure signals.

3. The neutron-pressure cross correlation technique can simply determine the sign of the void coefficient, thus determining in which zone the boiling occurs.

4. Despite the complicated boiling process, the neutron and pressure power spectra appear as one or more sine waves (with some bandwith) superimposed upon background noise.

5. Any correlation between the background noise sources and boiling can only aid the detection of boiling (cf.footnote on page 11).
6. Detection of local boiling in the zero void coefficient zone of an LMFBR will be very difficult unless other strong reactivity perturbation mechanisms exist.

It is the conclusion of this report that the neutron-pressure cross correlation technique is a serious alternative method for the detection of local boiling in sodium cooled reactors and that this method should be applied in future in-core sodium boiling experiments.

Appendix

| | |
|---|---|
| $\alpha_v$ | reactivity void coefficient |
| $\beta$ | delayed neutron fraction |
| $\delta(\omega)$ | fission chain noise source |
| $G(\omega)$ | reactivity feedback transfer function |
| $H(\omega)$ | zero power point reactor model reactivity transfer function |
| $\lambda$ | one group delayed neutron decay constant |
| $\Lambda$ | neutron generation time |
| $N_o$ | mean neutron population |
| $N'$ | neutron detector current minus the mean current |
| $\eta(\omega)$ | detection noise source |
| $P$ | $= P_B + P_L$ |
| $P_B$ | pressure input due to boiling |
| $P_L$ | pressure input due to power noise |
| $\rho$ | $= \rho_B + \rho_L$ |
| $\rho_B$ | reactivity input due to boiling |
| $\rho_L$ | reactivity input due to power noise |
| $j\omega$ | complex frequency |
| $S_{\delta\delta}(\omega)$ | $= \langle \nu(\nu-1) \rangle F$ |
| $S_{\eta\eta}(\omega)$ | $= W \overline{q^2} F$ |
| $T$ | averaging time |
| $V(\omega)$ | bubble volume |

When a parameter is written as a function of angular frequency, the fourier transform of the time signal is implied.

Bibliography

/1/ Lipinski W.C., Cohn C.E., and others:
Instrumentation Systems to Protect LMFBR Core Integrity
ANL-7793, March 1971

/2/ Schlechtendahl E.G.:
Sieden des Kühlmittels in natriumgekühlten schnellen Reaktoren
KFK 1020, EUR 4302 d, June 1969

/3/ Gast K.:
Die Ausbreitung örtlicher Störungen im Kern Schneller Natriumgekühlter Reaktoren und ihre Bedeutung für die Reaktorsicherheit
KFK 1380, May 1970

/4/ Schleisiek K.:
Natriumexperimente zur Untersuchung lokaler Kühlungsstörungen in brennelementähnlichen Testanordnungen
KFK 1914, Feb. 1974

/5/ Cronenberg A.W., Fauske H.K., and others:
A Single-Bubble model for Na Expulsion from a Heated Channel
Nuclear Engineering Design, 16, 285, 1971

/6/ Edelmann M.E., Ehrhardt J., and others:
Experiments for Development of Methods and Systems to Detect Sodium Boiling in an LMFBR
Nuclear Power Plant Control and Instrumentation,
IAEA-SM-168/E-3, 1973

/7/ Marciniak T.J., Habegger L.J., Greenspan H.:
Summary Review of Neutronic Noise Techniques for Incipient Boiling Detection in Liquid Metal Fast Breeder Reactors
ANL-7652, Jan. 1970

/8/ Bendat J.S.:
Principles and Applications of Random Noise Theory
New York, John Wiley and Sons, Inc., 1958

/9/ Uhrig R.E.:
Random Noise Techniques in Nuclear Reactor Systems
New York, The Ronald Press Company, 1970

| Neutronic Noise Sources | Acoustic Noise Sources |
|---|---|
| Reactor Control System | Primary Pump noise |
| Coolant flow turbulence | External pump noise (e.g. cover gas) |
| Inlet coolant temperature fluctuations | In-core Vibrations |
| Inherent noise due to the statistical nature of heat transfer and fission rate | Out-of-core Vibrations |
| In-core Vibrations | |

Table I Background Noise Sources for Acoustic and Neutronic Noise

| | Positive Void Coefficient | Negative Void Coefficient |
|---|---|---|
| $\omega << \beta/\Lambda$ | $+ 180^{o}$ | $0^{o}$ |
| $\omega >> \beta/\Lambda$ | $+ 90^{o}$ | $- 90^{o}$ |

Table II Neutron-Pressure CPSD Phase Angle as a Function of Frequency and Sign of the Void Coefficient

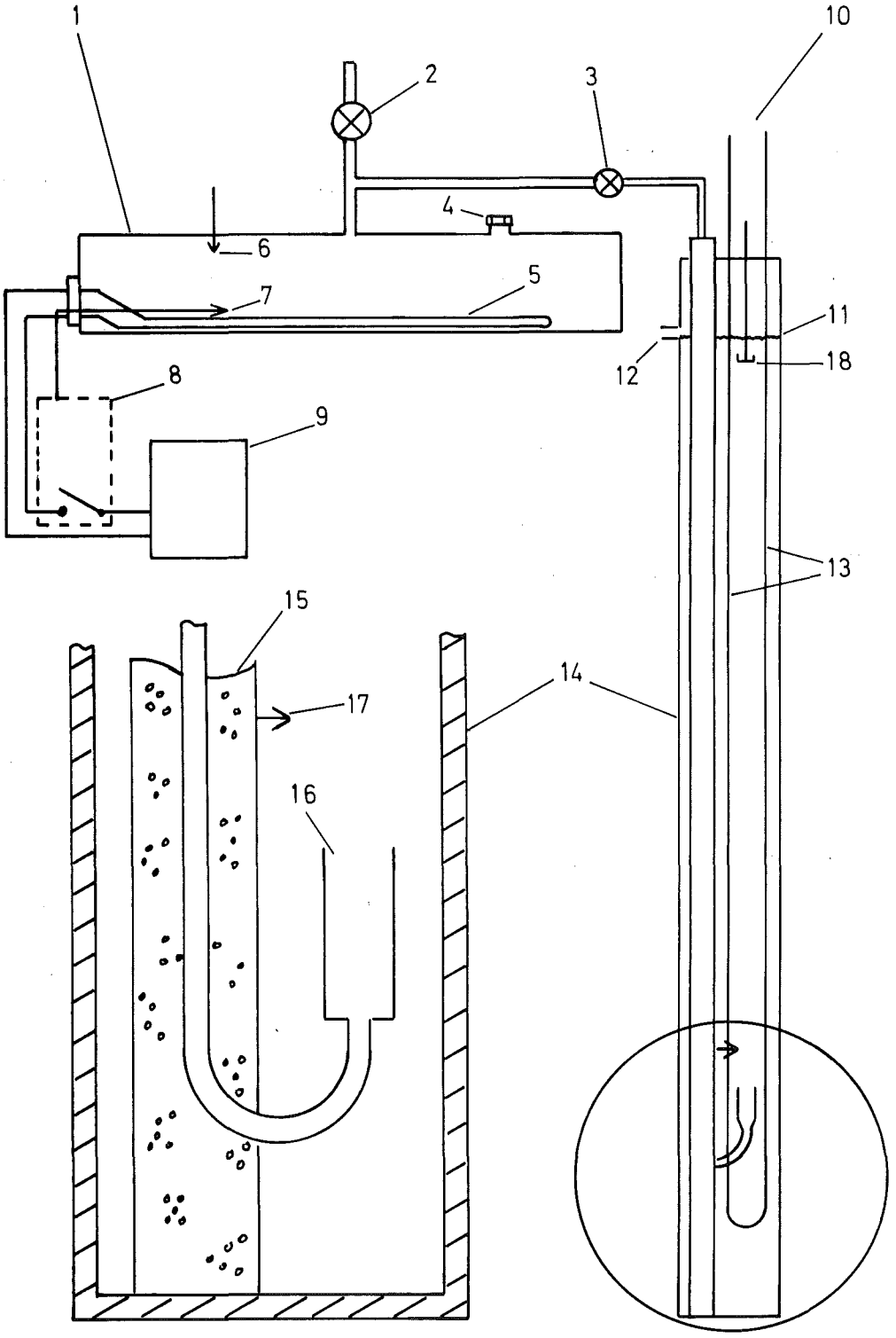


1 STEAM GENERATOR
2 SAFETY VALVE
3 STEAM VALVE
4 WATER INLET
5 HEATING ELEMENT
6 THERMOCOUPLE $T_s$
7 THERMOCOUPLE $T_h$
8 THERMOSTAT
9 TRANSFORMER
10 WATER COLUMN
11 WATER LEVEL
12 OVERFLOW
13 COOLING TUBES
14 PLEXIGLASS TUBE
15 TEFLON TUBE
16 NOZZEL
17 THERMCOUPLE $T_w$
18 PRESSURE DETECTOR

FIGURE 1 : BOILING SIMULATOR

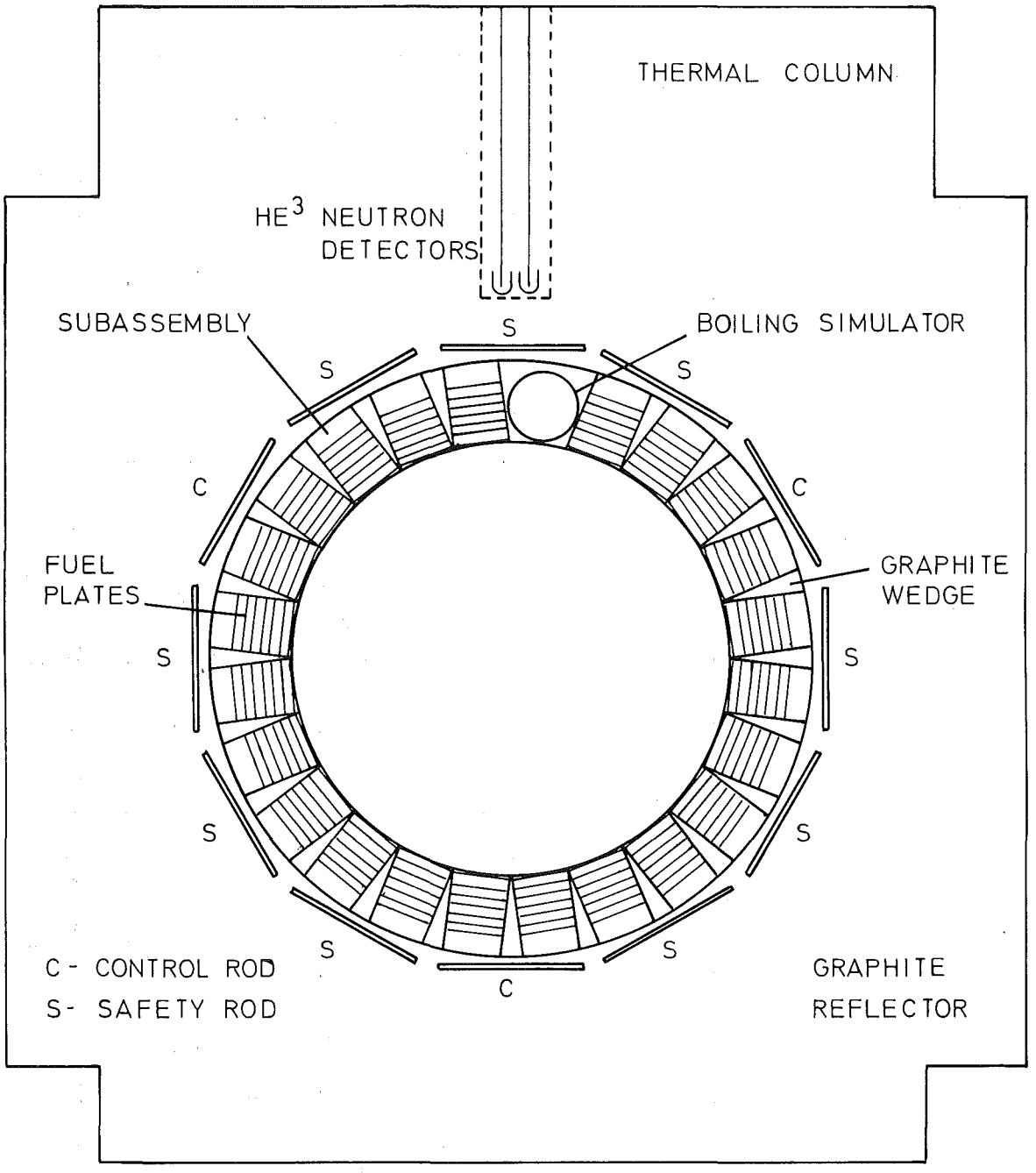


FIGURE 2 : GfK ARGONAUT REACTOR ARK

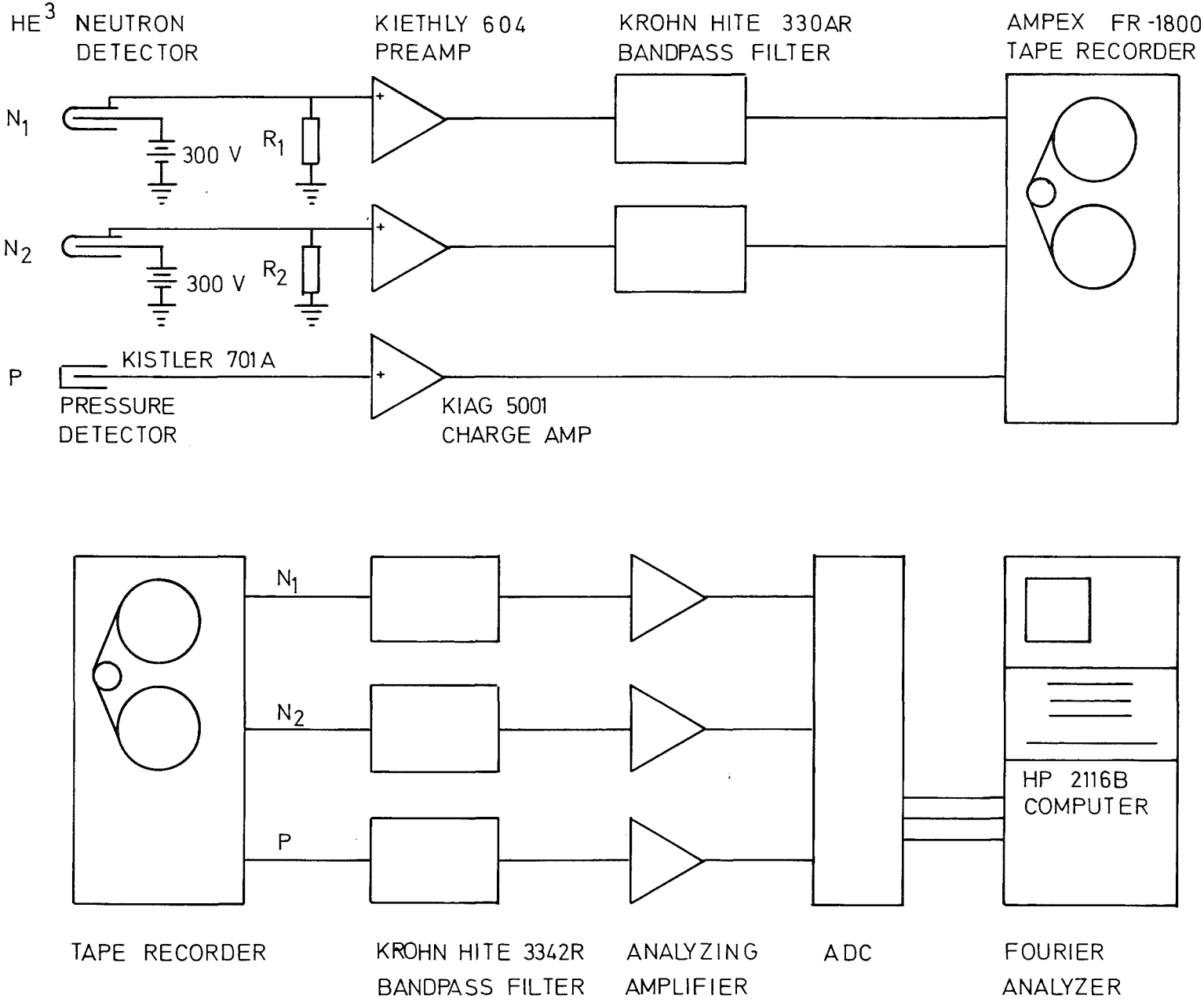


FIGURE 3 : ANALYSIS EQUIPMENT

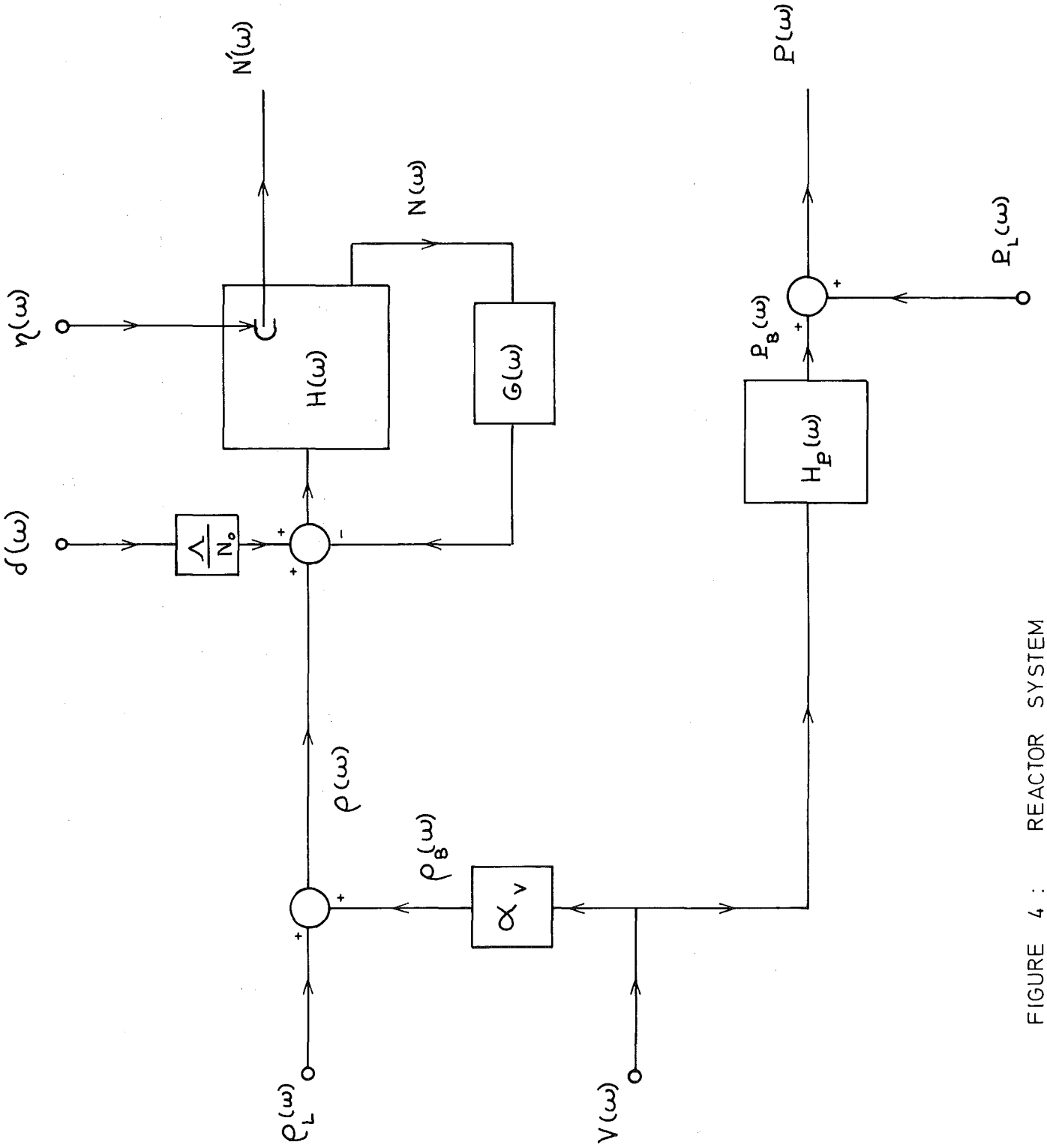


FIGURE 4 : REACTOR SYSTEM

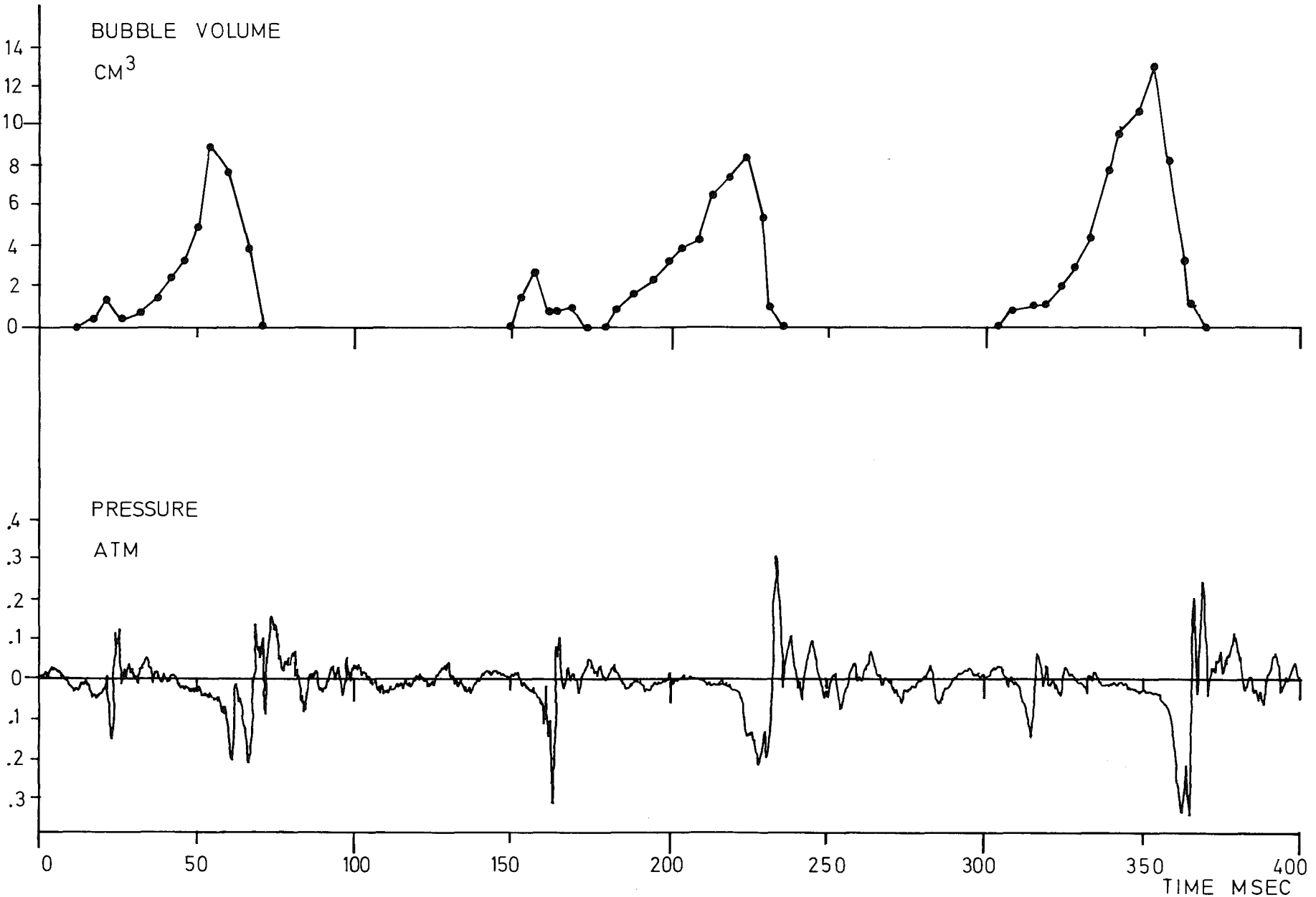


FIGURE 5 : BUBBLE VOLUME AND PRESSURE FROM SIMULATED LOCAL BOILING

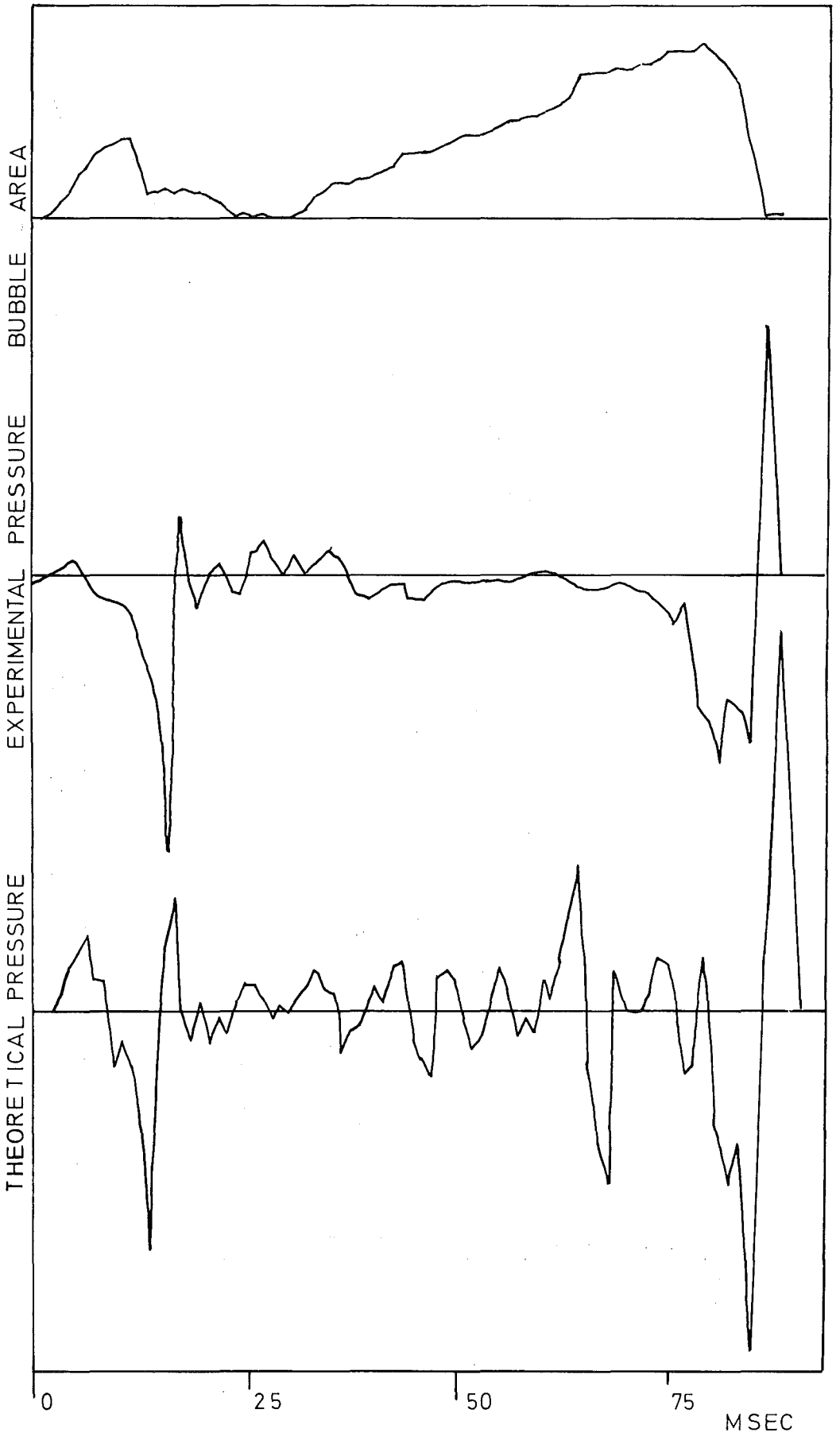


FIGURE 6 : MEASURED AND PREDICTED PRESSURE

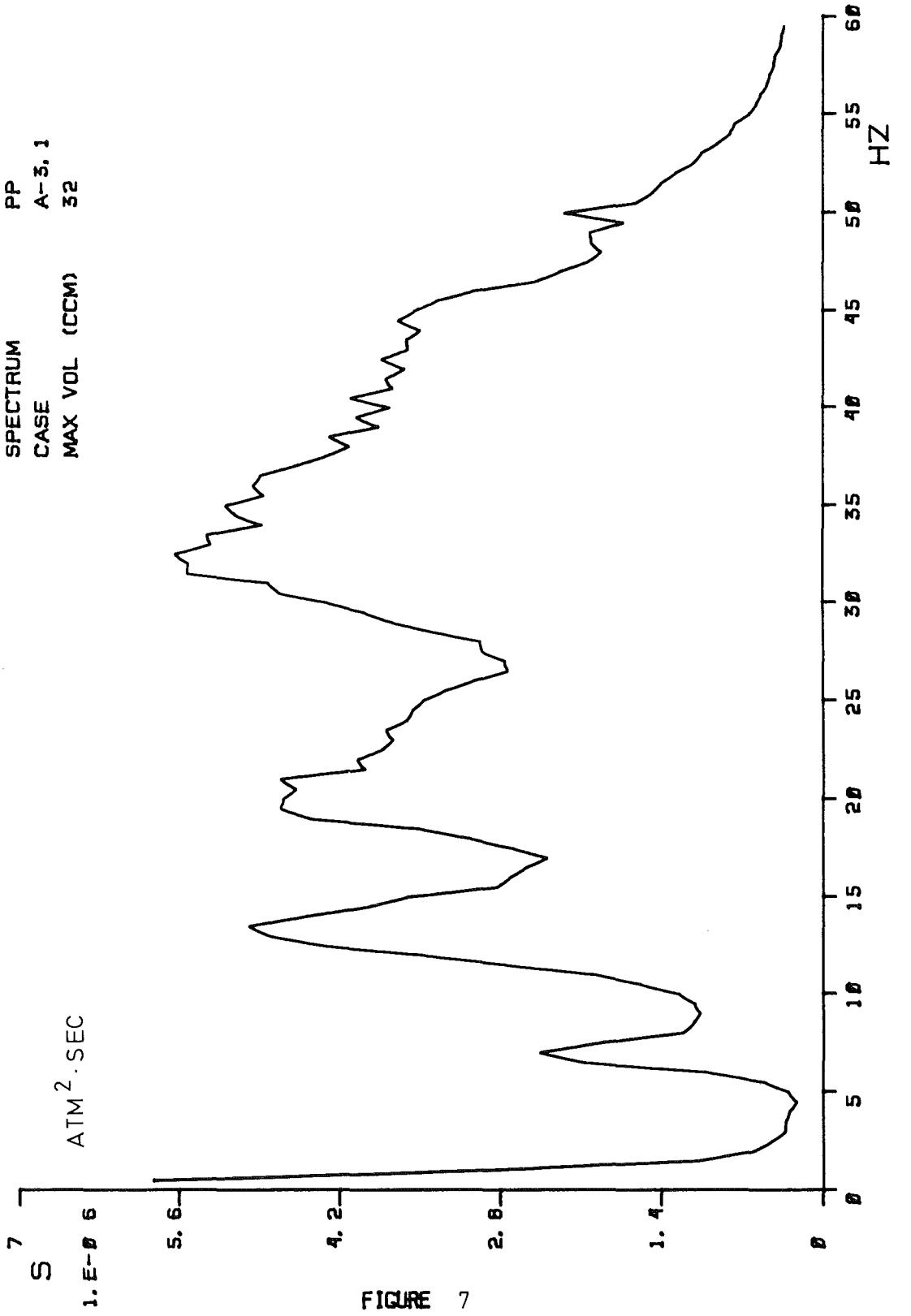
SPECTRUM PP
CASE A-3.1
MAX VOL (CCM) 32
S
ATM$^2$.SEC
1.E-0 6
5.6
4.2
2.8
1.4
0
0
5
10
15
20
25
30
35
40
45
50
55
60
HZ

FIGURE 7

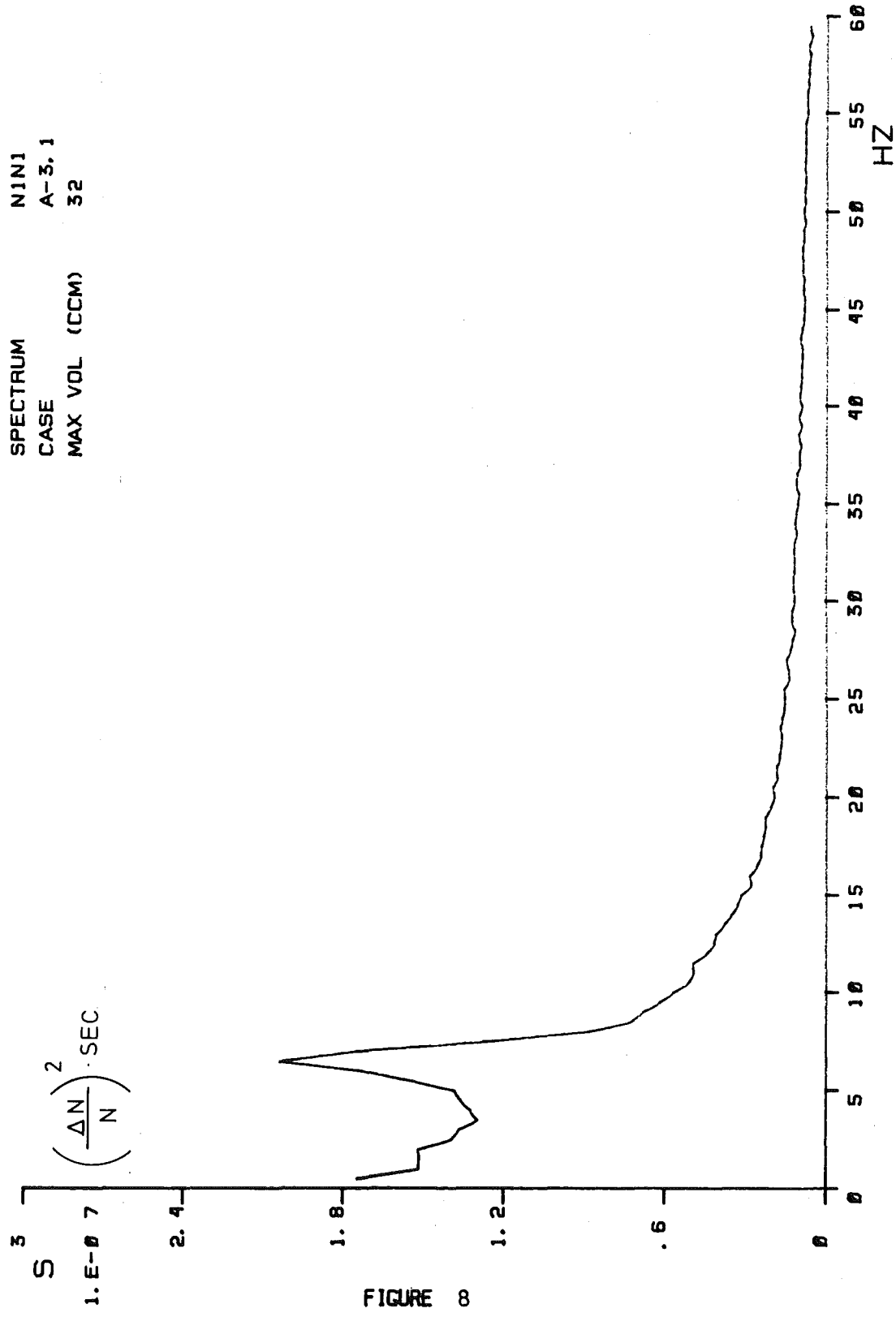
SPECTRUM N1N1
CASE A-3.1
MAX VOL (CCM) 32
S
1.E-07
$\left(\frac{\Delta N}{N}\right)^2 \cdot SEC$
3
2.4
1.8
1.2
.6
0
0
5
10
15
20
25
30
35
40
45
50
55
60
HZ

FIGURE 8

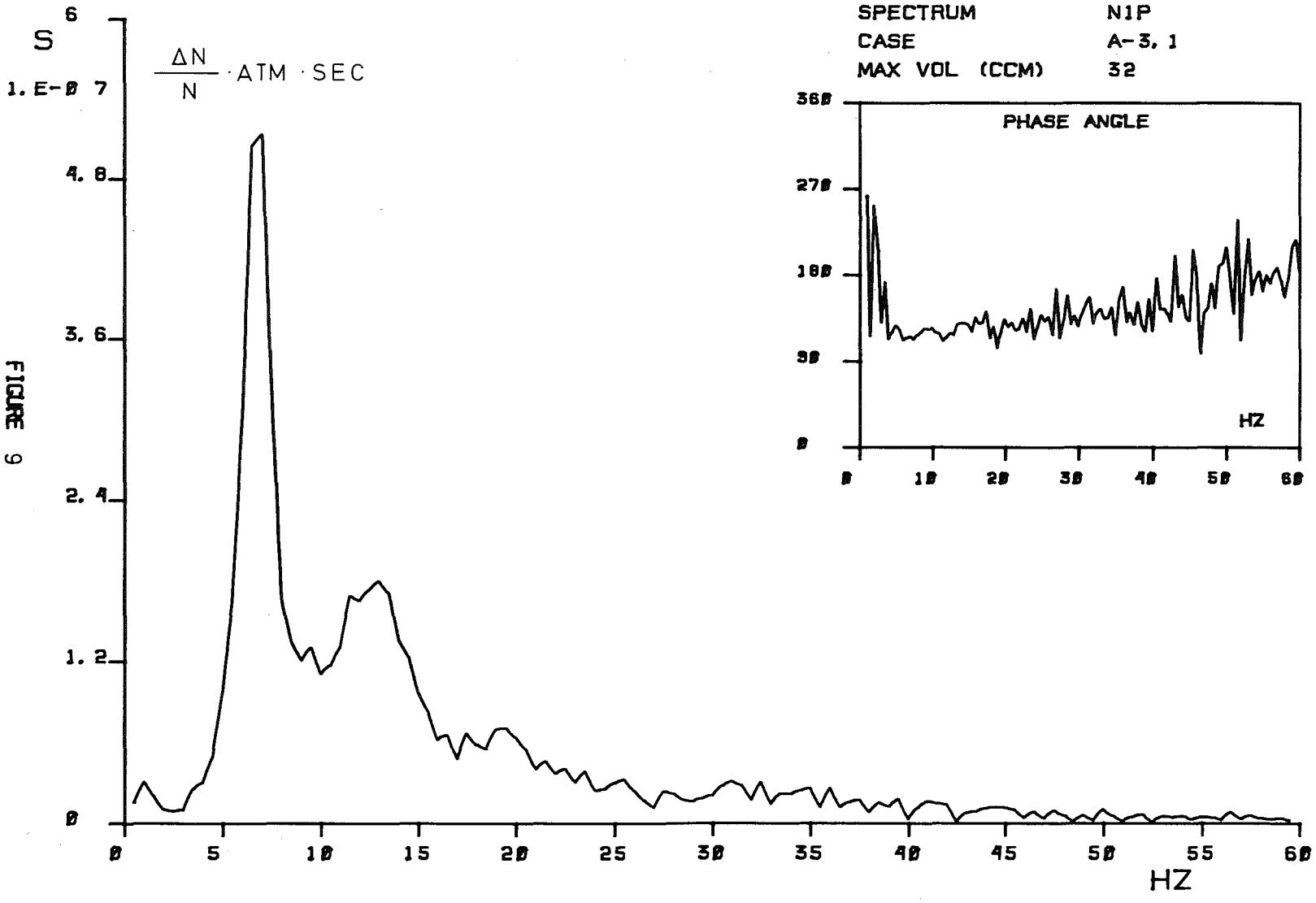
SPECTRUM N1P
CASE A-3, 1
MAX VOL (CCM) 32
PHASE ANGLE
HZ
S
ΔN/N · ATM · SEC
1.E-07
4.8
3.6
2.4
1.2
0
5
10
15
20
25
30
35
40
45
50
55
60
HZ

FIGURE 9

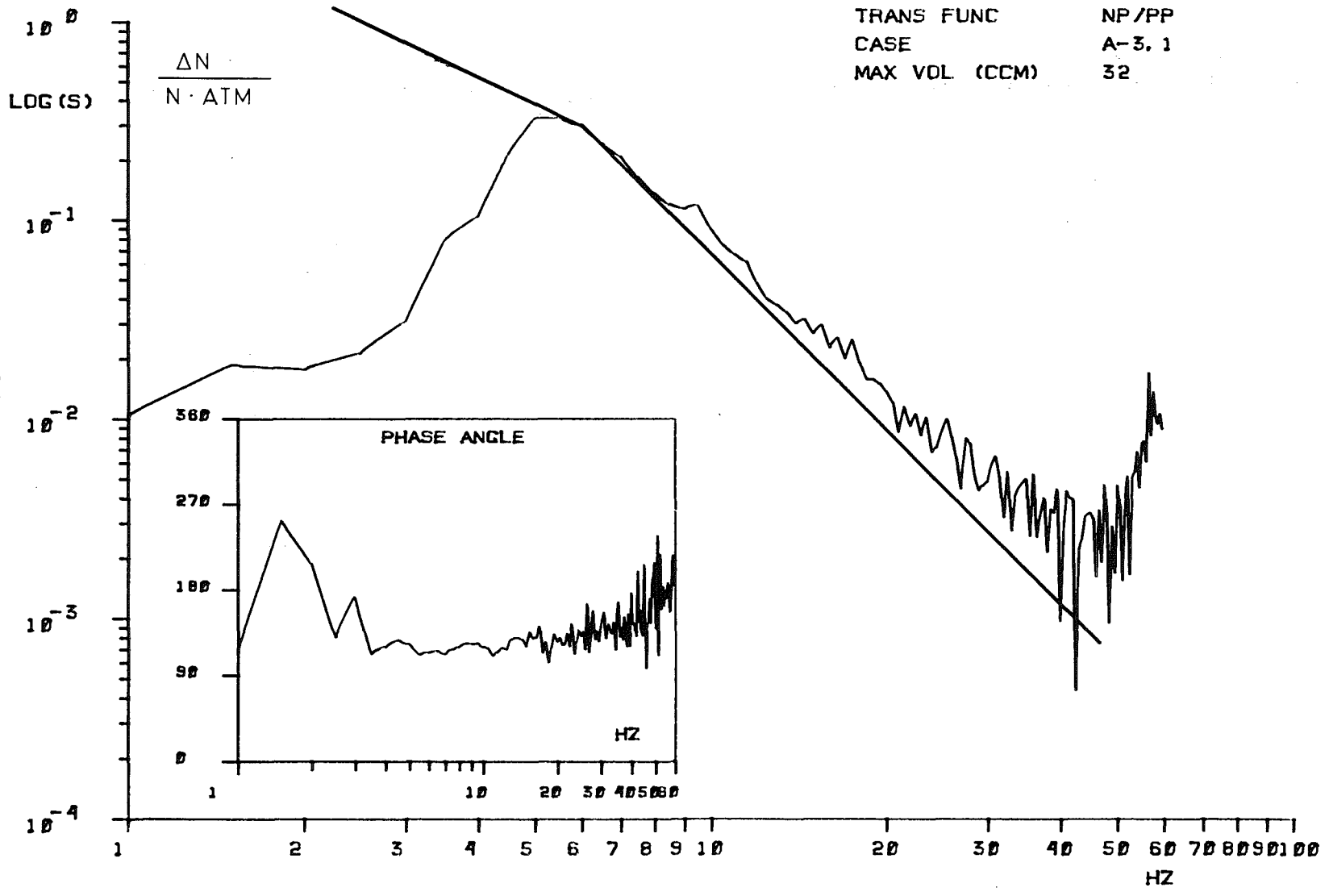
TRANS FUNC NP/PP
CASE A-3.1
MAX VOL (CCM) 32
ΔN / N · ATM
LOG (S)
10^0
10^-1
10^-2
10^-3
10^-4
PHASE ANGLE
360
270
180
90
0
HZ
1 10 20 30 40 50 60
1 2 3 4 5 6 7 8 9 10 20 30 40 50 60 70 80 90 100
HZ

FIGURE 10

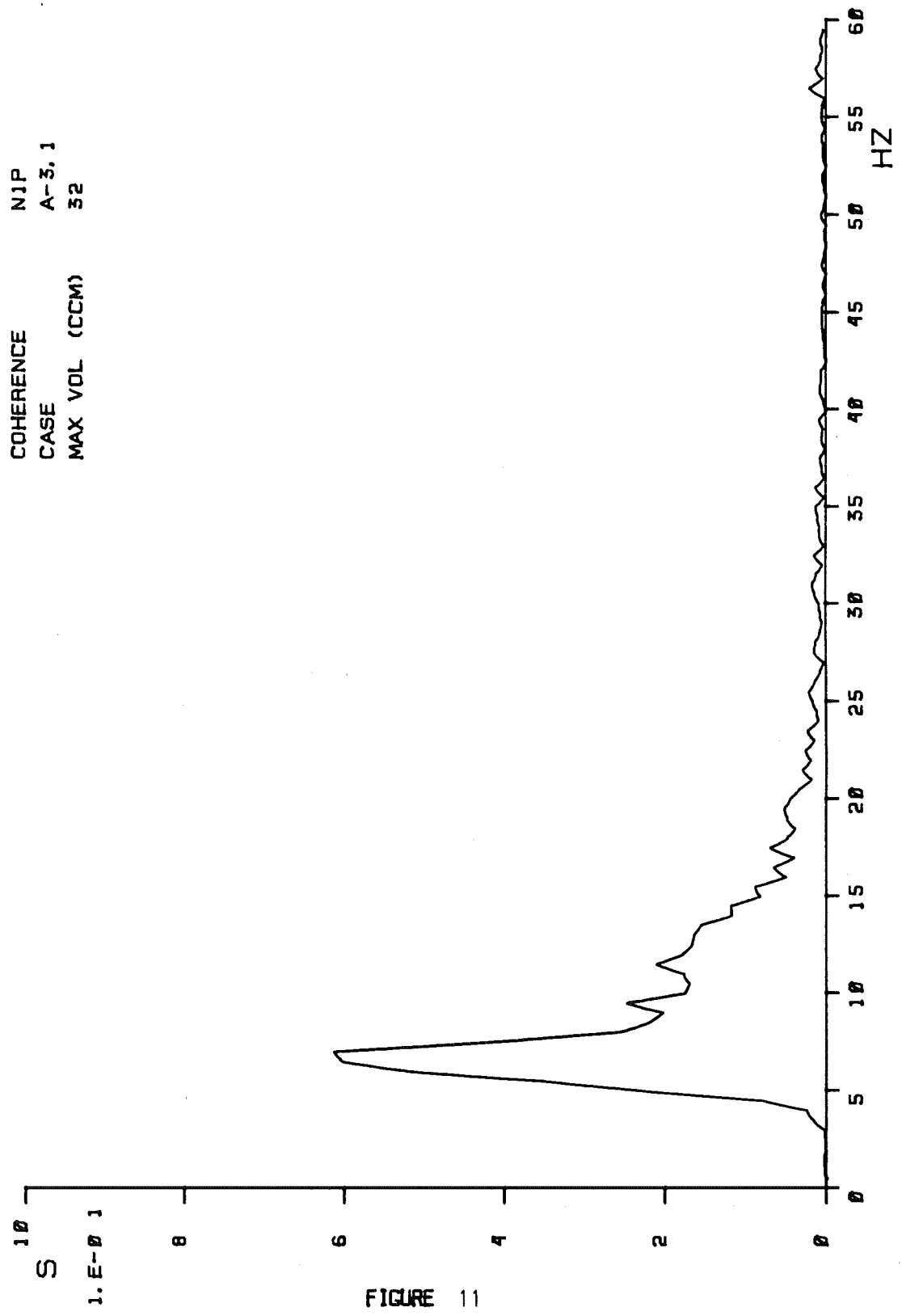
COHERENCE N1P
CASE A-3.1
MAX VOL (CCM) 32
S
1.E-01
10
8
6
4
2
0
0
5
10
15
20
25
30
35
40
45
50
55
60
HZ

FIGURE 11